Long-Range Interaction Forces between Polymer-Supported Lipid Bilayer Membranes

Markus Seitz,† Chad K. Park, Joyce Y. Wong,‡ and Jacob N. Israelachvili*

Department of Chemical Engineering, University of California, Santa Barbara, California 93106

Received February 26, 2001. In Final Form: May 3, 2001

Much of the short-range forces and structures of softly supported DMPC bilayers has been described previously. However, one interesting feature of the measured force−distance profile that remained unexplained is the presence of a long-range exponentially decaying repulsive force that is not observed between rigidly supported bilayers on solid mica substrate surfaces. This observation is discussed in detail here based on recent static and dynamic surface force experiments. The repulsive forces in the intermediate distance regime (mica−mica separations from 15 to 40 nm) are shown to be due not to an electrostatic force between the bilayers but to compression (deswelling) of the underlying soft polyelectrolyte layer, which may be thought of as a model cytoskeleton. The experimental data can be fit by simple theoretical models of polymer interactions from which the elastic properties of the polymer layer can be deduced.

Introduction

In recent years, lipid bilayer and model biomembranes supported on solid substrates have gained considerable attention as model systems for the fundamental study of biomembrane processes.[1−8] At the same time, technological and medical interest arises from their potential use as biosensors and models of biomembranes.[8−10] In this context, it is of considerable importance to attach a membrane to a substrate such that the supported membrane's natural hydrophilic environment, fluidity, and freedom are retained in order to conserve its biomimetic properties. While on hydrophilic oxidized silicon or silica a water layer (∼ a few angstroms thick) is formed which allows for free diffusion of phospholipid molecules within the bilayer,[11−13] on most other metal, metal oxides, and inorganic mineral surfaces, lipid mobility is strongly suppressed.[14,15] One promising and convenient approach is the use of water-swellable polymers for creating deformable and mobile substrates[8,16,17] that allow an aqueous layer several nanometers thick to separate the membrane from the underlying solid surface.

We have recently constructed phospholipid (DMPC) bilayers supported by a layer of branched polyethylenimine (PEI) on mica substrates by a two-step process in which small unilamellar lipid vesicles were adsorbed on preformed polymer-supported Langmuir−Blodgett (LB) lipid monolayers (Figure 1).[18] This allowed us to study the interaction forces, adhesion, and fusion of lipid bilayers in a more natural state employing the surface forces apparatus (SFA).[19] We found that the presence of the soft polymer cushion significantly alters the interaction between two bilayers, both the long-range force and the fusion pressure, when compared to solid- or rigidly supported systems. Thus, above the main transition temperature of DMPC bilayers ($T_m \approx 24$ °C), the activation pressure for hemifusion of softly supported bilayers is considerably smaller than for rigidly supported bilayers (i.e., directly supported on mica). After separation, softly supported membranes naturally reformed after short healing times. Also, for the first time, complete fusion of two fluid (liquid crystalline) phospholipid bilayers was observed in the SFA. Below T_m (in the gel state), very high pressures were needed for hemifusion and the healing process became very slow.[19]

In our earlier work, we focused on the effects of the polymer layer on the short-range interaction potential, but we also measured a long-range repulsive force that could not be explained by a purely electrostatic interaction. Furthermore, in structural investigations of our PEI-supported membrane system by neutron reflectivity, we were able to show a significant swelling of the polyelectrolyte cushion separating the lipid membrane from the substrate (quartz). When a PEI-supported DMPC mono-

† Current address: Lehrstuhl für Angewandte Physik, Ludwig-Maximilians-Universität, Amalienstrasse 54, 80799 München, Germany.

‡ Department of Biomedical Engineering, Boston University, 44 Cummington Street, Boston, MA 02215.

(1) Ti Tien, H. *Bilayer Lipid Membranes (BLM): Theory and Practice*; Marcel Dekker: New York, 1974.

(2) *Handbook of Biological Physics*; Lipowski, R., Sackmann, E., Ed.; Elsevier: New York, 1995.

(3) Ti Tien, H.; Ottova-Leitmannova, A. *Membrane Biophysics*; Elsevier: New York, 2000; Vol. 5.

(4) Tamm, L. K.; McConnell, H. M. *Biophys. J.* **1985**, *47*, 105−113.

(5) McConnell, H. M.; Watts, T. H.; Weis, R. M.; Brian, A. A. *Biochim. Biophys. Acta* **1986**, *864*, 95−106.

(6) Helm, C. A.; Israelachvili, J. N.; McGuiggan, P. M. *Science* **1989**, *246*, 919−922.

(7) Helm, C. A.; Knoll, W.; Israelachvili, J. N. *Proc. Natl. Acad. Sci. U.S.A.* **1991**, *88*, 8169−8173.

(8) Sackmann, E. *Science* **1996**, *271*, 43−48.

(9) Cornell, B. A.; Braach-Maksvytis, V. L. B.; King, L. B.; Osman, P. D. J.; Raguse, B.; Wieczorek, L.; Pace, R. J. *Nature* **1997**, *387*, 580−583.

(10) Raguse, B.; Braach-Maksvytis, V.; Cornell, B. A.; King, L. G.; Osman, P. D. J.; Pace, R. J.; Wieczorek, L. *Langmuir* **1998**, *14*, 648−659.

(11) Bayerl, T.; Bloom, M. *Biophys. J.* **1990**, *58*, 357−362.

(12) Johnson, S. J.; Bayerl, T. M.; McDermott, D. C.; Adam, G. W.; Rennie, A. R.; Thomas, R. K.; Sackmann, E. *Biophys. J.* **1991**, *59*, 289.

(13) König, S.; Sackmann, E. *Curr. Opin. Colloid Interface Sci.* **1996**, *1*, 78−82.

(14) Groves, J. T.; Ulman, N.; Boxer, S. G. *Science* **1997**, *275*, 651.

(15) Groves, J. T.; Ulman, N.; Cremer, P. S.; Boxer, S. G. *Langmuir* **1998**, *14*, 3347.

(16) Häussling, L.; Knoll, W.; Ringsdorf, H.; Schmitt, F. J.; Yang, J. L. *Makromol. Chem., Macromol. Symp.* **1991**, *46*, 145−155.

(17) Spinke, J.; Yang, J.; Wolf, H.; Liley, M.; Ringsdorf, H.; Knoll, W. *Biophys. J.* **1992**, *63*, 1667−1671.

(18) Wong, J. Y.; Majewski, J.; Seitz, M.; Park, C. K.; Israelachvili, J. N.; Smith, G. S. *Biophys. J.* **1999**, *77*, 1445−1457.

(19) Wong, J. Y.; Park, C. K.; Seitz, M.; Israelachvili, J. N. *Biophys. J.* **1999**, *77*, 1458−1468.

10.1021/la0103012 CCC: $20.00
Published on Web 06/23/2001

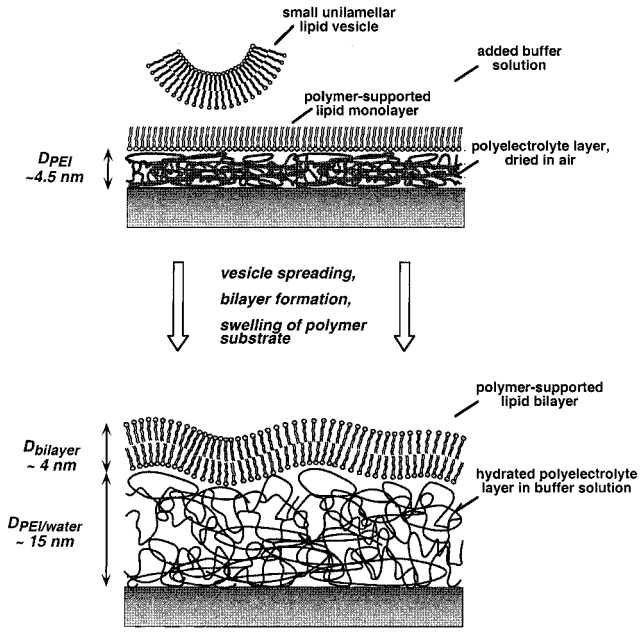

Figure 1. Preparation of polyelectrolyte-supported lipid bilayers by vesicle adsorption onto polymer-supported lipid monolayers. While the sketch is not intended to be fully drawn to scale, given values for the thickness of polymer and lipid layers, *D*, are from neutron reflectivity studies on quartz (cf. ref 18).

layer is first deposited onto quartz by the LB technique and then treated with a solution of small unilamellar DMPC vesicles in buffer solution, the thickness of the supporting polymer layer increases from 4.5 nm (supported monolayer in air) to ~15 nm (supported bilayer in buffer solution). At the same time, the polymer/water (v/v) ratio within the cushion decreases from $^1/_1$ to approximately $^1/_3$.[18]

In this paper, we will briefly summarize our earlier SFA studies and then describe recent experiments by which we could relate the long-range repulsion to the compression of the water-swollen polymer cushion. In dynamic SFA experiments, the viscosity of the liquid medium between the two surfaces can be measured.[20−22] From the viscosity profile, one can determine the position of the shear plane relative to the position of the solid surface ($D = 0$), which in turn can be related to the thickness of a fully immobilized hydrodynamic layer, such as a polymer layer. This method could therefore be used to probe the PEI-supported bilayer thickness on mica. In additional static experiments, we measured the normal interaction forces in an "asymmetric" setup, in which the two apposing bilayer systems are no longer identical. This allowed us to identify the nature of several individual contributions to the systems' interaction profile in more detail. These experimental results can be compared to simple theoretical models for the long-range repulsive contribution from which elastic properties of the polymer cushion supporting the lipid bilayer can be extracted.

Experimental Section

Mica surfaces coated with an interfacial layer of branched polyethylenimine ($M_w \approx 1800$ g mol^{-1}, 95% purity; Polysciences, Warrington, PA) were prepared by adsorbing the polymer from aqueous solution (100 ppm) at room temperature for at least 2 h followed by rinsing with MilliQ water. Note that commerically available, statistically branched polyethylenimines synthesized by cationic ring-opening polymerization of aziridines normally show a rather broad molecular weight distribution with primary, secondary, and tertiary amino units present in a ratio of 1:2:1. However, in low molecular weight (oligomeric) material as used here, the ratio between primary and tertiary amino units normally differs from 1:1 because of the use of termination reagents in the cationic polymerization of ethylenimine.[23−25] This synthetic process leads to short and nearly linear polymer chains, with one short side branch per approximately 3.5 repeat units along a linear polyethylenimine main chain.[25,26] The choice of this low molecular weight PEI with a low degree of branching is important to provide a homogeneous water-swollen layer on the mica substrate, while high molecular weight PEI has been found to absorb as a very patchy interfacial layer on charged surfaces.[27] For the preparation of PEI-supported DMPC bilayers on mica and quartz substrates, we could successfully employ the well-established formation of lipid bilayers by vesicle fusion on solid substrates[17,28−30] also on the soft polymer surfaces. The parameters governing the preparation process have been carefully evaluated in our previous work, and the polymer-supported bilayer structure was confirmed by structural characterization employing neutron scattering[18,19] and atomic force microscopy (AFM).[32] Briefly, the (proximal) DMPC monolayers were deposited at room temperature by LB transfer onto mica or quartz substrates from an aqueous subphase containing 100 ppm PEI and 0.5 mM KNO_3, and the formation of the second (distal) lipid layer could then be achieved by adsorption and fusion of small unilamellar vesicles onto the PEI-supported monolayers. The polymer adsorption conditions, namely, the salt concentration, were held constant in all preparations of PEI-supported DMPC monolayers, to ensure that always the same amount of polyelectrolyte was adsorbed to the substrate. For experiments with polymer-supported bilayers at conditions of varied electrolyte concentration (i.e., low salt, 0.5 mM KNO_3; high salt, 150 mM KNO_3), the salt content of the buffer was adjusted upon lipid vesicle adsorption. Hereby, the resulting lipid bilayer structures were found to depend on such factors as polymer hydration and salt concentration of the buffer.[18] Also, osmotic pressure acting on the lipid vesicles upon adsorption has been found to induce vesicle rupture and help to drive the formation of bilayers as opposed to the formation of vesicular aggregates adsorbed to the polymer-coated mica substrates. [32] Once established, this technique could be used in a convenient way for the preparation of polymer-supported lipid bilayers directly inside the SFA.[19] In a similar fashion, solid-supported lipid bilayers were prepared by adsorbing DMPC vesicles onto preinstalled crystalline DPPE monolayers on mica (prepared by LB transfer at room temperature from the solid-analogous monolayer phase).[28]

A detailed description of the SFA technique has been given elsewhere.[31] All bilayer preparations and SFA experiments described throughout the paper were carried out at 28 °C (i.e., above the gel−fluid phase transition temperature of DMPC bilayers, $T_m = 24$ °C). If not specified differently, in all force−distance curves shown in this paper, $D = 0$ corresponds to the contact of the bare mica substrates, which was determined before each experiment. Note that, as the disks had to be taken out of

(20) Israelachvili, J. N.; Kott, S. J.; Fetters, L. J. *J. Polym. Sci., Part B: Polym. Phys.* **1989**, *27*, 489−502.
(21) Horn, R. G.; Israelachvili, J. N. *Macromolecules* **1988**, *21*, 2836−2841.
(22) Klein, J.; Kamiyama, Y.; Yoshizawa, H.; Israelachvili, J. N.; Fredrickson, G. H.; Pincus, P.; Fetters, L. J. *Macromolecules* **1993**, *26*, 5552−5560.
(23) Jones, G. D.; MacWilliams, D. C.; Braxtor, N. A. *J. Org. Chem.* **1965**, *30*, 1994.
(24) Johnson, T. W.; Klotz, I. *Macromolecules* **1974**, *7*, 149−153.
(25) Dick, C. R.; Ham, G. E. *J. Macromol. Sci., Chem.* **1970**, *4*, 1301.
(26) Lukovkin, G. M.; Pshezhetsky, V. S.; Murtazaeva, G. A. *Eur. Polym. J.* **1973**, *9*, 559.
(27) Akari, S.; Schrepp, W.; Horn, D. *Langmuir* **1996**, *12*, 857−860.
(28) Kalb, E.; Frey, S.; Tamm, L. K. *Biochim. Biophys. Acta* **1992**, *1103*, 307−316.
(29) Lang, H.; Duschl, C.; Grätzel, M.; Vogel, H. *Thin Solid Films* **1992**, *210/211*, 818−821.
(30) Steinem, C.; Janshoff, A.; Ulrich, H.-P.; Sieber, M.; Galla, H.-J. *Biochim. Biophys. Acta* **1996**, *1279*, 169−180.
(31) Israelachvili, J. *Intermolecular and Surface Forces*, 2nd ed.; Academic Press Ltd.: London, 1991.
(32) Seitz, M.; Ter-Ovanesyan, E.; Hausch, M.; Park, C. K.; Zasadzinski, J.; Zentel, R.; Israelachvili, J. N. *Langmuir* **2000**, *16*, 6067−6070.

the SFA for the monolayer deposition, the *absolute* zero position is known only to an accuracy of ±0.5 nm. This yields a somewhat ambiguous thickness for the underlying polymer layer, but this experimental error is by an order of magnitude smaller than the typical deviations obtained for the layer thicknesses in our fitting procedures. Note that the relatively measured distances in the force profile are known to greater accuracy, typically 0.2 nm. For the measurement of intersurface forces ("static" force measurements), the motor compressing/separating the two surfaces was driven in steps of approximately 4 nm to measure the forces between the surfaces during compression and separation. At each step, an average time of ~5 s was needed to measure the actual intersurface separation. Therefore, in the range where no considerable force was acting between the surfaces, the average compression/expansion rate was ~1 nm/s. In the range where larger interbilayer forces were present, naturally the compression rate drops whereas the force loading rate remained constant (with a spring constant $K \approx 300$ N/m, a radius $R \approx 1.5$ cm, $\mathrm{d}(F/R)/\mathrm{d}t \approx 20$ μN/(m s)).

For the determination of the viscosity of the medium between the mica surfaces, the forces are measured when the surfaces are in relative motion ("dynamic" force measurements).[20,21] The upper surface oscillates around an average position, and the response of the lower surface is measured by detecting the "oscillating" mica−mica separation. This can be done either by decreasing the intersurface separation continuously (combination of sinusoidal and linear movement of the upper surface) or by a discontinuous procedure in which the average distance is decreased in steps and then held constant during the oscillation of the upper surface. For driving frequencies below 3 Hz, the movement of the fringe pattern can be monitored with a video camera and recorded on a videocassette recorder for later analysis. The amplitude of oscillation of the intersurface separation, A_D, is then measured from these recordings using a video micrometer. The driving frequency in the continuous and discontinuous measurements described here was $\nu_o = 0.1$ Hz. In the discontinuous measurements, the driving amplitude at each separation was chosen to be approximately 10% of the intersurface separation ($A_o \approx 0.1D$). The time for each measurement at each separation was on the order of 10 cycles (i.e., total time of measurement at each position, $10T = 10/\nu_o = 100$ s). In the continuous measurements, the surfaces were driven with an average speed of $v = 1-1.5$ nm/s, and the upper surfaces were oscillated with a typical amplitude of $A_o \approx 10-15$ nm.

The theoretical background for the evaluation of the experimental data has been given in the literature.[20,21] Briefly, the viscosity of the liquid at any mean separation, D, is given by

$$\eta = K(1 - \nu^2/\nu_o^2)D[(A_o/A_D)^2 - (1 - f/K)]^{1/2}/12\pi^2R^2\nu \quad (1)$$

where K is the spring constant of the lower support, ν and ν_o are the driving frequency of the upper surface and the resonant frequency of the lower surface, respectively, R is the radius of the crossed cylindrical surfaces, A_o and A_D are the respective amplitudes of the oscillating motion of the upper surface and of the intersurface separation, and f is the gradient of the static force at the mean intersurface separation D. When $\nu \ll \nu_o$ and in the absence of any static force between the surfaces, eq 1 simplifies to

$$\eta = KD[(A_o/A_D)^2 - 1]^{1/2}/12\pi^2R^2\nu \quad (2)$$

Thus, for a Newtonian liquid, a plot of $12\pi^2R^2\nu/\{K[(A_o/A_D)^2 - 1]^{1/2}\}$ versus D should be a straight line passing through the origin (if the shear plane is at $D = 0$) whose inverse slope gives the viscosity η of the liquid. Polymer layers adsorbed onto the mica surfaces can be idealized as a totally immobilized layer of thickness Δ_H (hydrodynamic layer thickness) by which the effective plane of shear is shifted (e.g., for polymer layers of the same thickness Δ_H on each mica surface, $D = 2\Delta_H$).

Results

Symmetric Case: Static and Dynamic Interaction Forces between PEI-Supported DMPC Bilayers. *Static Force Measurements: Short-Range Forces (Summary of Previous Studies).* An important feature of the investigated PEI-supported DMPC membranes is the significant amount of water taken up by the polyelectrolyte support. This gives rise to a considerable aqueous compartment between the substrate and the lipid bilayer that contains only 15−20 vol % of the polymer as indicated by previous neutron reflectometry studies.[18] It was found in previous static SFA measurements on these systems[19] that the presence of the polymer cushion allows the lipid membrane to exist in a mobile state above the phase transition temperature (i.e., $T_m \approx 24$ °C for DMPC) which significantly alters the interaction potential between the two membranes. The temperature dependence of the measured interaction profile as well as the hemifusion and healing of softly supported membranes was also discussed in this context. The major implications of that previously published work are as follows:[19]

(1) For the first time, both hemifusion and complete fusion of two interacting lipid bilayers was observed in the SFA. Above T_m, the activation pressure to achieve hemifusion was found to be considerably small ($F/R \approx 20$ mN m^{-1}, i.e., $P_{planar} \leq 10$ atm). After separation from the hemifused state, complete healing of the membranes was observed which suggested that the fluidity of the system was preserved on the PEI cushion. The mobility of lipid molecules within a polymer-supported lipid membrane was also studied by fluorescence microscopy.[48] While no full FRAP setup was available, the diffusion constants within the fluid bilayer membrane could nevertheless be roughly estimated from the fluorescence recovery of a photobleached spot in a DMPC bilayer carrying 0.5 mol % of a TR-DHPE probe lipid and were found to be at least $D_{min} \approx 0.1\,\mu$m^2 s^{-1} but no higher than $D \approx 5\,\mu$m^2 s^{-1}. While this is a very crude estimate, it allows us to estimate a maximum healing time for a contact region in the SFA experiment with a typical diameter of $d \approx 20$ μm as $t_{max} \approx 1$ h, which is the approximate time of a full compression−separation cycle in the SFA experiments. Also, full fusion of two fluid phospholipid bilayers was observed in the SFA for the first time. Below T_m, that is, when the DMPC bilayer was in the gel state, very high pressures were needed for hemifusion and the healing process became very slow. These results were in striking contrast to earlier results on the fusion of solid-supported bilayers,[6,33,34] where hemifusion could only be realized in lipid systems with packing defects (e.g., bilayers with specific weak points such as grain boundaries), for bilayers with dissolved solvents or heterogeneous bilayers such as "egg PC", and under extremely high pressures of up to $P = 50-100$ atm.[33,34] The observations on PEI-supported DMPC bilayers, however, did agree with temperature-dependent fusion studies of large contacting unilamellar vesicles,[35,36] which further indicated that the polymer-supported systems resemble the behavior of free lipid membranes in solution.

(2) The abrupt change in thickness found upon hemifusion of two membranes was a direct measure of the lipid bilayer thickness (including a layer of hydration water). The measured bilayer dimensions in the SFA experiments on PEI-supported DMPC membranes agreed well with literature-reported X-ray data on multilamellar DMPC bilayer stacks,[37] which were also confirming our observed thickening of DMPC bilayers at lower temperatures ($T <$

(33) Horn, R. G. *Biochim. Biophys. Acta* **1984**, *778*, 224−228.
(34) Helm, C. A.; Israelachvili, J. N.; McGuiggan, P. M. *Biochemistry* **1992**, *31*, 1794−1805.
(35) Breisblatt, W.; Ohki, S. *J. Membr. Biol.* **1975**, *23*, 385−401.
(36) Ohki, S. In *Membrane Fusion Techniques, Part A.*; Düzgünes, N., Ed.; Academic Press: San Diego, CA, 1993; pp 79−89.

T_m). As this effect occurred in the expected temperature range of the gel−fluid phase transition of the DMPC bilayer, that is, in measurements just above (28 °C) and below (21 °C) the transition, it is another stong indicator that the aqueous compartment provided by the water-swollen polyelectrolyte cushion allows the lipid membrane to exist in a nearly unperturbed natural state.

(3) No significant adhesion was measured when two interacting unfused bilayers surfaces were separated ($E_{ad} \approx 0.02$ mJ m^{-2}).[19] This again was in striking contrast to studies on solid-supported bilayers, where significant adhesive energies up to 0.6 mJ m^{-2} were determined upon separating two contacting lipid membranes.[47] Again, the conserved fluidity in PEI-supported DMPC membranes makes them more comparable with free bilayer vesicles; in fact, the measured adhesion energies were found to be nearly identical to those determined from vesicle adhesion measurements[38] or by the micropipet aspiration technique.[39] Interestingly, no adhesion was observed even upon separating two previously hemifused bilayers. As the separation of two membrane leaflets in water should certainly be accompanied by a significant hydrophobic energy, this observation may be an indication of very fast recovery of the lipid membranes upon separation (and/or a very weak interaction between membranes and polymer cushions).

Static Force Measurements: Long-Range Interactions. An interesting observation in these previous studies was that the measured repulsive force decayed with a characteristic length of ~10 nm at mica−mica separations D > 20 nm, stretching out to approximately 50 nm.[19] However, measured forces were too high to be explained by the DLVO theory for a purely electrostatic interaction. In addition, the repulsive behavior at higher monovalent salt concentration (150 mM KNO_3) did not differ much from the low-salt case (Figure 2); that is, no screening of the repulsive interaction was observed in the intermediate distance regime (20−40 nm). Instead, the determined decay length was slightly increased ($\lambda^{-1} \approx 12$ nm).[40] The static interaction forces during the expansion of the surfaces followed those measured on compression (i.e., no hysteresis) when only moderate forces were applied (F/R < 10 mN/m, D > 11 nm). Interestingly, increasing compressive forces brought about increasingly hysteretic behavior; that is, the forces measured during separation were considerably smaller and shorter-ranged than those measured on compression. The effect was greatest in the separation curves after previous hemifusion or fusion events (during which compression forces up to ~20 mN/m were applied) and manifested itself by significantly steeper decay lengths of the repulsive force in the separation curves (detailed data are not shown, but also cf. Figure 4B for a qualitative illustration on this effect). On the other hand, there has been no indication of a strong dependence of the hysteresis on the time the lipid bilayer surfaces were kept in contact, but further experiments would be needed in order to quantify this effect.

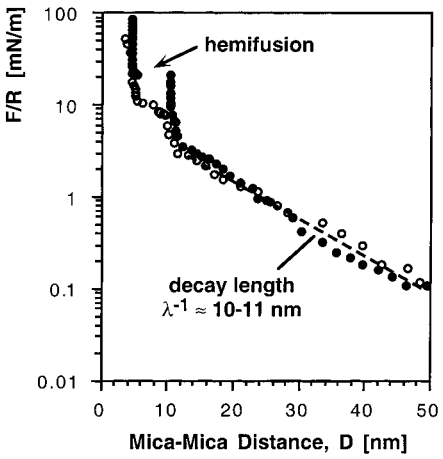

Figure 2. Interaction profiles of two mica surfaces covered with PEI-supported lipid bilayers at 28 °C under conditions of low and high salt concentration (static SFA experiment, symmetric case, cf. ref 19). Full dots: high salt concentration (0.5 mM KNO_3); open symbols: low salt concentration (150 mM KNO_3).

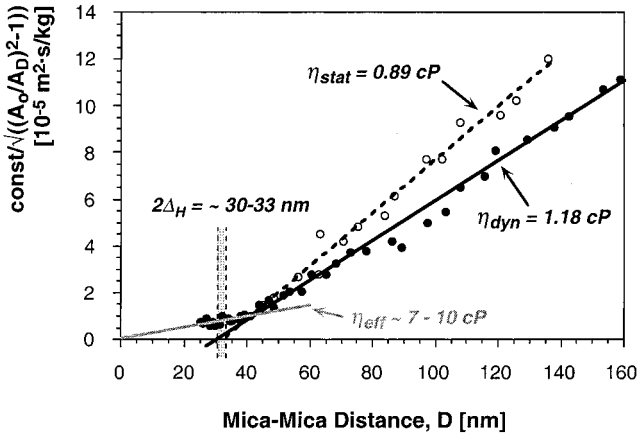

Figure 3. Determination of hydrodynamic layer thickness of PEI-supported DMPC bilayer membranes at 28 °C in dynamic SFA experiments. Open dots: discontinuous (static) approach (fitted by dashed black line); filled dots: continuous (dynamic) approach (fitted by straight black line); gray line: fit to regime in which bilayer surfaces are in contact.

Dynamic Force Measurements. The experimental data obtained in dynamic force measurements using an oscillating driving function for the upper surface are plotted in Figure 3 as $12\pi^2R^2\nu/\{K[(A_o/A_D)^2 - 1]^{1/2}\}$ versus D. According to eq 2, the determination of the effective viscosity of the medium between the two mica surfaces is obtained as the inverse slope of the linear regime of the plots. While for bare substrates a straight line passing through the origin $D = 0$ would be expected, the presence of permanently immobilized layers on each surface shifts the x-intercept of the fitted lines by $D = 2\Delta_H$.

The data for both discontinuous and continuous approaches of the surfaces give straight lines above D > 40 nm. In this regime, the static force between the two PEI-supported bilayers is less than F/R < 0.1 mN/m, and eq 2 is sufficient to describe the response of the lower surface. The viscosity of the medium between the two surfaces is found to be $\eta_{stat} = 0.89$ cP for the discontinuous ("quasi-static") approach and $\eta_{dyn} = 1.18$ cP for the continuous (completely dynamic) approach. These numbers correlate well with the expected viscosity of the 0.5 mM KNO_3 buffer solution separating the two interacting bilayers (note that

(37) In the previous SFA study of the fusion process of polymer-supported membranes, the thickness of a DMPC bilayer in the fluid state was determined as $D_B = 3.5$ nm. The thickness of a hydrated DMPC bilayer was estimated as $D_B + D_W \approx 5.7$ nm from the hemifusion process. The thickness of two contacting DMPC bilayers thus includes one layer of hydration water, that is, $2D_B + D_W \approx 9.2$ nm (cf. ref 19). These numbers are in good agreement with earlier X-ray studies by Janiak et al. where $D_B = 3.55$ nm and $D_B + D_W \approx 6.0$ nm were obtained (cf.: *Biochemistry* **1976**, *15*, 4575−4580).

(38) Bailey, S. M.; Chiruvolu, S.; Israelachvili, J. N.; Zasadzinski, J. A. *Langmuir* **1990**, *6*, 1326−1329.

(39) Evans, E.; Needham, D. *J. Phys. Chem.* **1987**, *91*, 4219−4228.

(40) Note that the different salt conditions were introduced during the bilayer preparation inside the SFA apparatus, while LB transfer of PEI-supported monolayers was always performed at 0.5 mM KNO_3. Therefore, the conditions for PEI adsorption were the same in both cases.

under these low electrolyte conditions employed the effect of dissolved KNO_3 on the buffer's viscosity can be neglected and that $\eta_{H_2O} = 0.83$ cP at 28 °C for pure water). The two straight lines fitting the data in the long-range regime intersect the distance axis at approximately 30−33 nm. From this, the hydrodynamic layer thickness of one PEI-supported bilayer on mica can be estimated as $\Delta_H \sim 16 \pm 1$ nm. In the regime of $D < 40$ nm, significant static forces F/R are measured. For $D < 20$ nm ($F/R > 1$ mN/m), the oscillating of the intersurface separation becomes considerably damped ($A_D < 1$ nm) and was thus no longer accurately measurable. The obtained data can be fitted to give a straight line, although with less accuracy as compared to the long-range regime (note that the error introduced by using the simplified eq 2 is still well below 5%). The resulting viscosity number is increased by an order of magnitude ($\eta_{eff} \approx 7-10$ cP) between $D = 20$ and 40 nm.

Asymmetric Cases: Static Interaction Force Measurements. To elucidate the contribution of the polymer cushion to the long-range repulsion between softly supported lipid membranes, two asymmetric static experiments were designed which will be presented in the next two sections, namely, a PEI-supported DMPC bilayer versus mica covered with PEI absorbed from solution (case I) and a PEI-supported DMPC bilayer versus a solid-supported bilayer of DMPC on DPPE (case II).

Asymmetric Case I: Polymer-Supported Bilayer versus Bare Polymer Substrate. As a control, two polymer-supported DMPC bilayers were repeatedly measured confirming our previous observed interaction profiles (Figure 4B, curve a). Then, the asymmetric experiment was set up by replacing the upper of the two surfaces with a bare PEI-coated mica substrate (left sample sketched in Figure 4A). This yields two distinctive changes in the interaction profile (Figure 4B, curve b). The steric barrier (hard wall, D_{hw}), resulting from contact between the two surfaces, was shifted to lower distances by approximately the thickness of one DMPC bilayer ($\Delta D_{hw} = 3.8$ nm).[37] Also, the long-range repulsive interaction extended further out than for the symmetric case (with $\lambda^{-1} \approx 12$ nm), and the observed hysteresis was more pronounced.

After repeated contact of the two surfaces in successive measurements of the same contact region, a second bilayer formed on the bare polymeric substrate. This was indicated by a continuous recovery of the steric barrier for bilayer−bilayer contact at $D = 10.5$ nm, accompanied by an increase of the F/R value required for hemifusion until it nearly reached the originally observed hemifusion barrier of two interacting PEI-supported DMPC bilayers (Figure 4B, curve c). Interestingly, it seems that contact or flattening of the surfaces (or both) are important requirements for bilayer formation on the bare polymer layer. Despite the presence of free DMPC vesicles in solution, we never observed bilayer formation on the bare polymeric substrate on first approach even after a long waiting time (hours) following the exchange of the upper surface or after changing to a fresh position on the bare polymer surface. Finally, expansion curves show typical hysteresis as discussed above. Hysteresis is more significant in curve b (open circles).

Asymmetric Case II: Solid-Supported versus Polymer-Supported Bilayers. In contrast to the previous experiments, the repulsive interaction range was drastically decreased when a system of two lipid bilayers and only one polymer layer was investigated. Particularly, the system of a PEI-supported DMPC bilayer and a solid-supported lipid bilayer (Figure 5A) was formed by adsorption of small unilamellar vesicles onto preformed

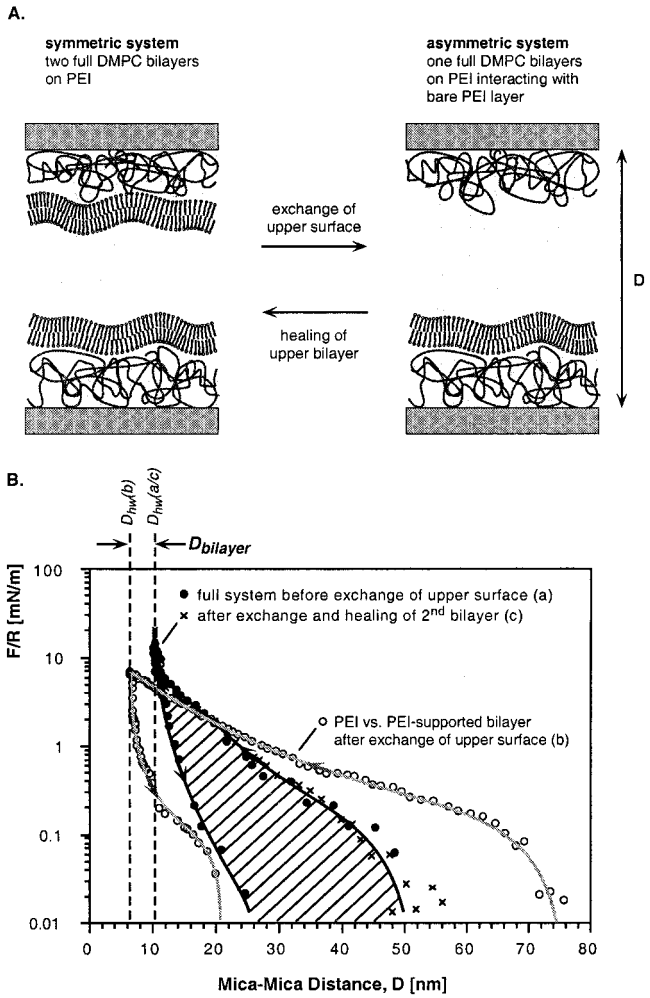

Figure 4. Interaction profiles of a PEI layer on mica with a PEI-supported DMPC bilayer membrane at 28 °C in 0.5 mM KNO_3 solution (static SFA experiment, asymmetric case I). A system of two PEI-supported bilayers was measured first (full symbols) followed by an exchange of the upper surface by a bare polymer layer on mica. Open symbols are the interaction profile measured immediately after exchanging the upper surface (asymmetric force profile). With time and repeated contact of the surfaces, the upper surface "healed" (as indicated by the crossed symbols).

monolayers of DMPC on PEI/mica and DPPE on mica, respectively. As shown in Figure 5B, the decay length of the measured exponential repulsion, $\lambda^{-1} \approx 2.5$ nm, is significantly smaller than for the case of two polymer-supported membranes (by a factor of 4). In addition, at $F/R \approx 0.4$ mN/m a kink (or short plateau region) is observed in the curve which may be related to an adhesion between the two lipid membrane surfaces. The adhesive energy can be determined from the jump out of contact in the expansion curve as $W_{ad} \approx 0.17$ mJ/m^2.

Fit Results. The experimental data were fitted by several equations based on simple theoretical models. First of all, a simple exponential fit was used,[31,41]

$$F/R = A \exp(-\lambda D) \qquad (3)$$

Here, A is a general parameter and λ is the decay length of the repulsive interaction.

Second, a simple spring model introduced by Kühner and Sackmann[42] was modified for our particular system

(41) Mondain-Monval, O.; Espert, A.; Omarjee, P.; Bibette, J.; Leal-Calderon, F.; Philip, J.; Joanny, J. F. *Phys. Rev. Lett.* **1998**, 1778−1781.

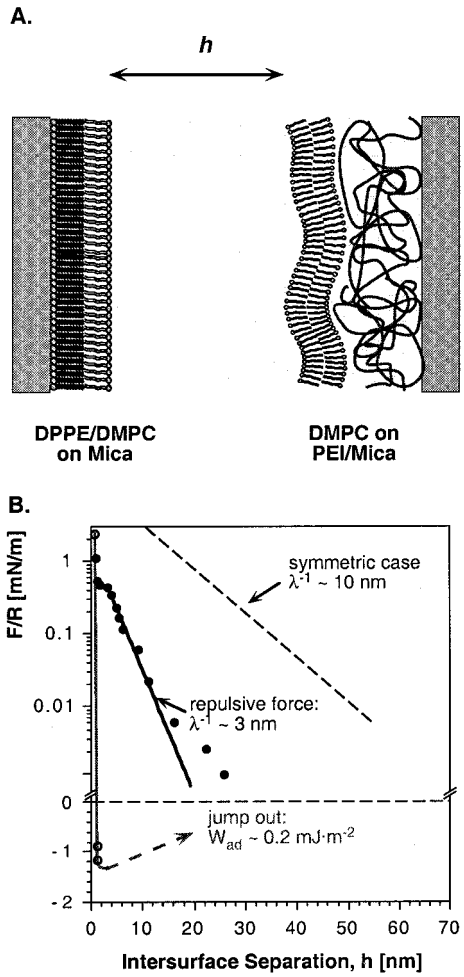

Figure 5. Interaction profile of a solid-supported bilayer of DPPE/DMPC on mica with a PEI-supported DMPC bilayer membrane at 28 °C in 0.5 mM KNO_3 solution (static SFA experiment, asymmetric case II). Full symbols: compression; open symbols: expansion data. Here, forces are plotted against the intersurface separation h (i.e., the zero position, $h = 0$, is defined for the two bilayer surfaces in contact) in order to allow for a better comparison with the symmetric case (as indicated by the dashed line).

(see Appendix). The polymer cushion is treated as an elastic continuum being compressed along the z-axis. This allows the extraction of an effective Young's modulus, E_{eff}, of the polymer substrate.[43] Also, the effective total thickness, $D^{(o)}$, of the interfacial layers (polymer + lipid) is obtained from the fit, from which the total thickness of the polymer cushions, $D_p{}^{tot}$, can be deduced.

$$F/R = \pi E_{\text{eff}}(2D^{(o)} - D)^2/D_p{}^{tot} \qquad (4)$$

Finally, to get further quantitative structural information on the system, the Alexander−de Gennes equation[44,45]

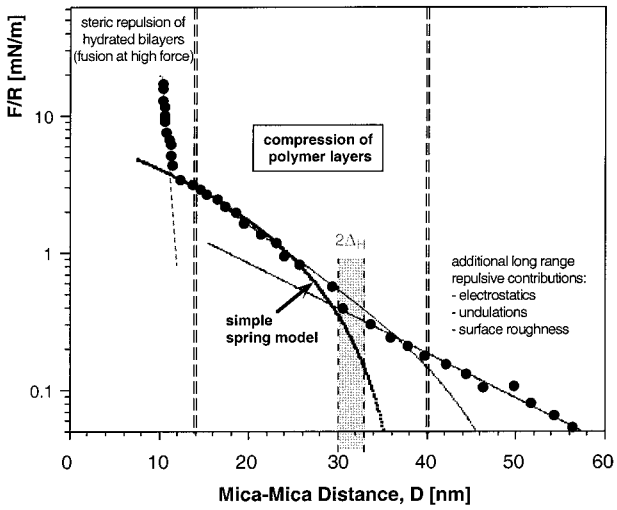

Figure 6. Full interaction profile of two PEI-supported DMPC bilayers on mica substrates (T = 28 °C, 0.5 mM KNO_3).

was also used to model the experimental data. In eq 5, next to the total layer thickness, $D^{(o)}$, the grafting density of the polymers at the surfaces is represented by the mean distance between two grafting sites, s, which can also be deduced from the fit.

$$F(D)/R = \frac{8k_BT\pi D^{(o)}}{35s^3}\left[7\left(\frac{D^{(o)}}{D}\right)^{5/4} + 5\left(\frac{D}{D^{(o)}}\right)^{7/4} - 12\right] \qquad (5)$$

Although developed specifically to model terminally grafted polymer brushes, the form of the resulting steric force (osmotic force) is very similar for end-grafted or adsorbed polymer layers at lower surface densities. The model can be successfully applied to fit the repulsive interaction forces between other "swollen" interfacial layer systems such as, for example, microemulsion droplets on surfaces.[46] Equation 5 therefore seems to be a good general description of the interaction force in terms of an osmotic repulsion and elastic energy for separation distances smaller than the overall thickness of the surface layers, $D^{(o)}$. However, note that bridging interactions are still ignored, and thus the forces at larger separation are typically still underestimated (but apparently to a somewhat lesser extent than the simple spring model as will be seen below).

Figure 6 shows the interaction profile of two PEI-supported DMPC bilayers fitted by the different models. The short-range interaction for $D < 14$ nm (resulting from the steric repulsion of the two contacting surfaces) can be fitted by an exponentially decaying force of characteristic length $\lambda^{-1} \approx 0.85$ nm. However, the simple exponential fit gives different results for the intermediate ($D \approx 15-40$ nm) and long-range regimes ($D > 40$ nm). In general, there is good agreement between experimental data and theoretical curves obtained from eqs 3−5 in the regime of intermediate distances and at intermediate forces ($F/R \approx 0.5-3$ mN/m). It is noted, however, that the theoretical curve of the simple spring model (bold curve in Figure 6) drops to zero force at smaller values of the mica−mica separation, D, than the fit curve according to the Alex-

(42) Kühner, M.; Sackmann, E. *Langmuir* **1996**, *12*, 4866−4876.

(43) Note that a macroscopic model considering elastic deformations of the interacting layers has also been discussed in ref 42, in which the interacting layers were described as deformable continuous half spaces according to the Hertz theory (cf.: Hertz, H. *J. Reine Angew. Math.* **1881**, *92*, 156−171). Higher Young's moduli (by an order of magnitude) were obtained for such a macroscopic approach. However, the finite thickness of the polymer layers is ignored by such an approach. Particularly, the thickness of the real polymer cushions is on the order of the size of one hydrated polymer molecule, such that the microscopic point of view can be regarded to be more reliable. We follow this argument but give the obtained elastic moduli as effective Young's moduli, E_{eff}, to reflect their dependence on the theoretical assumptions of the simple spring model.

(44) de Gennes, P. G. *C. R. Acad. Sci.* (*Paris*) **1985**, *300*, 839−843.

(45) Kamiyama, Y.; Israelachvili, J. *Macromolecules* **1992**, *25*, 5081−5088.

(46) Giasson, S.; Kuhl, T. L.; Israelachvili, J. N. *Langmuir* **1998**, *14*, 891−898.

Table 1. Fit Results of Static Interaction Forces between DMPC Bilayer Membranes Based on Simple Theoretical Models (Equations 3−5)

	exponential fit	simple elastic model		Alexander−de Gennes fit	
	λ^{-1} [nm]	D_p^{tot}[nm][a]	E_{eff} [10^3 N m^{-2}]	D_p^{tot}[nm][a]	s [nm]
Symmetric Cases					
PEI/DMPC vs DMPC/PEI, 0.5 mM KNO_3, low salt (I)	9.5 ± 1.1	29.2 ± 1.2	47.0 ± 4.8	45.4 ± 2.6[b]	11.1 ± 0.6
PEI/DMPC vs DMPC/PEI, 150 mM KNO_3, high salt (II)	11.7 ± 0.7	32.9 ± 2.5	32.1 ± 6.9	58.4 ± 11.6[b]	14.3 ± 2.4
Asymmetric Cases					
PEI vs DMPC/PEI, 0.5 mM KNO_3 (III)	11.3 ± 0.8	38.6 ± 2.7	42.8 ± 7.5	84.3 ± 5.5[b]	17.2 ± 1.0
DPPE/DMPC vs DMPC/PEI, 0.5 mM KNO_3 (IV)	2.5 ± 0.4	12.4 ± 2.4	34.7 ± 10.4	11.3 ± 1.7[c]	10.8 ± 2.1

[a] The total thickness $D^{(o)}$ as obtained from the fit is correlated with the total polymer layer thickness by $D_p^{tot} = D^{(o)} - D_{Lip}$. For cases I and II, $D_{Lip} = 2D_{DMPC} + D_W \approx 9.2$ nm; for case III, $D_{Lip} = D_{DMPC} \approx 3.5$ nm. In case IV, instead of the mica−mica distance, D, the surface separation $h = 0$ is defined for bilayer−bilayer contact (cf. Figure 5B). Thus, $D_p^{tot} = D^{(o)} + D_{PEI\ compressed} \approx D^{(o)} + 0.5$ nm (cf. ref 19). [b] $D_p^{tot} = 2D_p^{(o)}$ [c] $D_p^{tot} = D_p^{(o)}$

ander−de Gennes model (gray curve). Generally, a lower thickness for the two bilayer systems is obtained from the spring model; here, $F/R = 0$ mN/m at $D^{(o)} = 38.4$ nm for the spring model as compared to $D^{(o)} = 54.6$ nm from the Alexander−de Gennes fit.

The fit results in the intermediate regime for all measured interaction profiles (the symmetric case for both high as well as low salt conditions and the two asymmetric cases at low salt) and for all three models are summarized in Table 1.

Discussion

The starting point of the described experiments was the observation of a long-range repulsive interaction in a symmetric setup of two PEI-supported DMPC bilayers in 0.5 mM KNO_3 solution.[19] At mica−mica separations $D >$ 20 nm, the repulsive force falls exponentially with a characteristic decay length of $\lambda^{-1} \approx 10$ nm. Typically, such a behavior could be attributed to electrostatic interactions arising from the surface charge on either the PEI or the mica substrate (or the bilayer surfaces). At first sight, the measured data agree fairly well with the expected Debye length of an electrostatic interaction which at the given electrolyte concentration would be $\kappa^{-1}_{(theoret)} = 13.6$ nm.[31] However, the absolute observed repulsive forces are too high to be explained by DLVO theory, unless a significant shift of the layer of effective charge ("Stern layer") away from each mica surface is considered. In addition, if the long-range exponential repulsive interaction in the range from $D \approx 20$ to 50 nm were purely electrostatic in origin, the decay length should be greatly decreased at higher electrolyte concentration ($\kappa^{-1}_{theoret} = 0.8$ nm for 150 mM KNO_3). This was not observed in the experiments, as the observed decay length remained nearly unchanged (Figure 3), and the approximate agreement with the Debye length at 0.5 mM KNO_3 appears to be merely coincidental. Second, the time scale of the molecular processes underlying the observed hyseresis in the intermediate force range must be on the order of the time scale of the SFA experiment (several minutes). Because ionic diffusion in aqueous solution is a much faster process, the observed interaction in the hysteretic regime can therefore not be explained by electrostatics alone. Finally, the presence of small unilamellar DMPC vesicles is discounted as a source of the long-range force. In control experiments, the prepared surfaces were extensively rinsed with KNO_3 solution before their installation into the SFA. The measured interaction profile was essentially identical to measurements in which DMPC vesicles were present in solution. On the basis of this observation, it can be assumed that the influence of free vesicles in solution is negligible and not responsible for the observed long-range repulsion. Further, the neutron results do not show evidence of adhering vesicles on the bilayer surfaces.[18] We are thus left to conclude that the long-range forces above $D >$ 20 nm originate from the compression of the underlying polyelectrolyte cushions. Direct proof for this assumption was obtained from the asymmetric SFA experiments.

The results of the second set of asymmetric SFA experiments (case II, solid vs softly supported lipid bilayer, Figure 5) clearly show that the long-range repulsive interaction observed in polymer-supported bilayer systems must indeed be related to the water-swollen polyelectrolyte cushion. The long-range repulsive force is decreased, both in strength (magnitude) as well as in range ($\lambda^{-1} \approx 2.5$ nm) by "removal" of one PEI cushion. Also, the observation of adhesive jumps out of contact in this asymmetric experiment can be related to the decreased fluidity and flexibility of solid-supported lipid bilayers, as it has been discussed earlier.[19,47,48] Note that the almost complete absence of such instabilities for two interacting "soft" bilayer systems correlates well with the notion of a continuous unbinding of two adhering membranes when thermal fluctuations are allowed.[49,50]

From our earlier neutron scattering experiments on quartz supports, the thickness of the PEI cushion was determined as $D_p \approx 14.4$ nm when DMPC vesicles were adsorbed onto polymer-supported DMPC monolayers prepared by Langmuir−Blodgett deposition.[18] Upon addition of the vesicle solution, the thickness of the polymer layer increased by a factor of ~3.3 (from initially 4.3 nm after drying in air) accompanied by a significant uptake of water. This earlier study gave important structural proof of the successful bilayer formation by vesicle adsorption on quartz substrates. However, the nature of the substrate is expected to have a significant effect on polyelectrolyte adsorption. Therefore, the thickness of the supporting PEI layer on mica and thus the total thickness of the polymer-supported bilayer system studied in the SFA experiments described here remained somewhat uncertain. The dynamic measurements described in this paper allowed the direct determination of the PEI layer thickness in the SFA. The measured hydrodynamic layer thickness, $\Delta_H \approx 16 \pm 1$ nm, agrees well with the neutron studies on quartz from which the total thickness of a PEI-supported DMPC bilayer was estimated as 18.7 ± 0.5 nm.[18] Also, from Figure 3, the viscosity of the interacting bilayer

(47) Marra, J.; Israelachvili, J. *Biochemistry* **1985**, *24*, 4608−4618.
(48) Seitz, M.; Park, C. K.; Wong, J. Y.; Israelachvili, J. N. In *Supramolecular Structure in Confined Geometries*; Warr, G., Manne, S., Eds.; ACS Symposium Series 736; American Chemical Society: Washington, DC, 1999; pp 215−230.
(49) Lipowski, R.; Leibler, S. *Phys. Rev. Lett.* **1986**, *56*, 2541.
(50) Evans, E. *Langmuir* **1991**, *7*, 1900−1908.

system in buffer solution can be determined and is found to increase significantly at mica−mica distances below $D < 50$ nm. In this distance regime, the static repulsive long-range forces can be fitted well by both the simple spring model and the Alexander−de Gennes equation (Figure 6).

Apparently, the Alexander−de Gennes model gives a better fit over a longer distance range. However, the resulting values for the total interfacial layer thickness, $D^{(o)}_{AdG}$, appear too high when compared with the experimentally determined total hydrodynamic layer thickness. Considering the values given in Table 1 for the symmetric system of two PEI-supported DMPC bilayers in 0.5 mM KNO_3 solution, the total thickness of the system as obtained from the spring model fit, $D^{(o)}_{spring} = 29.2 \pm 1.2$ nm, closely matches the value from the dynamic SFA studies, $2\Delta_H = 32 \pm 2$ nm. On the other hand, the value obtained from the Alexander−de Gennes fit, $D^{(o)}_{AdG} = 45.4 \pm 2.6$ nm, correlates with the onset of the viscosity increase in the dynamic measurements (Figure 3). Although this agreement could be coincidental, it may be argued that the purely elastic spring model appears to underestimate the repulsive forces at larger distances at which the suppression of interfacial conformational flexibility within the polymer and lipid layers should result in a (weak) entropic repulsion.

In the interaction profile of one PEI-supported DMPC membrane with a mica sample carrying only a preadsorbed polyelectrolyte layer (case I), the long-range repulsive interaction is still present and extends out to even larger distances. Apparently, the "free" polyelectrolyte layer can stretch out into solution more fully than the bilayer-covered PEI layer. In other words, the free PEI surface exists in a more hydrated (i.e., diluted) state when unconfined by the lipid membrane, which results in a longer-ranging steric interaction between the two surfaces, for example, by bridging effects.[51−57] In a similar way, the observed increase in the hysteretic behavior may be understood.

Conformational rearrangements in the polymer adsorption layer should affect the steric interaction forces dramatically and perhaps also water release and uptake from the polymer cushion upon compression/expansion of the system. Large hysteresis effects and history-dependent surface forces are well-known for polyelectrolyte-coated substrates.[58,59] It has been argued that slow relaxation processes of polyelectrolyte adsorption layers under compression are a result of conformational changes in the polymer layer and that the kinetics of this process is limited by the cooperative reorganization of local electrostatic bonds at the surface. As the observed force hysteresis of two interacting PEI-supported bilayers should be appreciable to the time scale of the measurement (seconds to minutes), it seems critical that for high molecular weight polyelectrolytes the relaxation times of this reorganization can amount up to several days.[59] However, considering the low molecular weight of the PEI used in our measurements, the relaxation to the equilibrium conformation after previous compression may proceed much faster.

Another possible explanation of the hysteretic behavior is related to the observed unusually high thickness of the PEI cushion. Note that in most previous SFA investigations on polyelectrolyte adsorption layers, much smaller layer thicknesses were observed, and long-range interaction forces could typically be attributed to electrostatic double-layer forces.[59−61] A hydrated PEI layer thickness of ∼15 nm is certainly much more than what would be expected for monolayer surface coverage with single adsorbed and flat-lying polyelectrolyte chains and even slightly higher than the highest possible value which would be obtained if the PEI chains would stand "upright" and adopt a fully stretched conformation upon hydration of the polymer film. The maximum layer thickness that could be achieved for a monolayer of fully stretched chains of slightly branched PEI with M_w ∼1800 g/mol would be ∼11 nm. But more likely, a bloblike conformation of the polymers should be found in the adsorption layer, and for an expanded polymer coil of this length, a Flory blob radius of only R_F ∼3.6 nm would be expected.[19] Although this is neglecting any further expansion of the blob because of electrostatic interactions between individual segments, the 15 nm thickness of the hydrated layer can by no means be explained by single monolayer coverage. We can only speculate at this point whether the excessive PEI surface coverage thickness might be the result of the LB deposition process (during which not only PEI molecules adsorbed to the mica substrate but also those attached to the DMPC monolayer would be transferred) or related to some other unique adsorption properties of the low molecular weight PEI under the conditions applied in our preparations. However, as neutron reflectometry suggests a water content of at least 80 vol % in the swollen PEI layer[18] and as the surface grafting densities of $s \approx 10-15$ nm determined from the Alexander−de Gennes fits indicate that less than one segment per present PEI chain should be interacting with the substrate, it appears that the swollen PEI cushion merely resembles a confined film of a concentrated aqueous polymer solution rather than a tightly surface-bound polymer monolayer. Earlier findings, in which it was observed that the compression of polyelectrolyte adsorption layers of polyallylaminehydrochloride (PAH) would result in an irreversible deformation of polyelectrolyte double layers at compressive forces beyond 10 mN/m,[61] may be consulted to further elaborate this notion. As the forces applied here exceed this value, this should let us expect lateral movement within the adsorption layers, which is further supported by the fact that only a very thin remaining adsorption layer was observed for a fully fused PEI-supported DMPC bilayer system (0.5−1.0 nm).[19] This lateral movement of the polymers in the PEI cushion may not only account for the observed hysteresis but should also be affecting the healing behavior of the lipid bilayer membrane (although the latter depends primarily on the phase state of the lipid bilayer). To fully explore these arguments, a more elaborate time- and force-dependent study of the expansion curves would be needed, which has not yet been done (the slowest overall separation speeds applied so far were at the order of 0.1 nm/s; i.e., one point on the expansion curve was recorded every 30 s so that the overall time for surface separation was approximately 25 min).

(51) Luckham, P. F.; Klein, J. *Macromolecules* **1985**, *18*, 721−728.
(52) Almog, Y.; Klein, J. *J. Colloid Interface Sci.* **1985**, *106*, 33−44.
(53) Dahlgren, M. A. G.; Claesson, P. M.; Audebert, R. *J. Colloid Interface Sci.* **1994**, *166*, 343.
(54) Claesson, P. M.; Paulson, O. E. H.; Blomberg, E.; Burns, N. L. *Colloids Surf., A* **1997**, *123−124*, 341−353.
(55) Poptoshev, E.; Rutland, M. W.; Claesson, P. M. *Langmuir* **2000**, *16*, 1987−1992.
(56) Dedinaite, A.; Claesson, P. M. *Langmuir* **2000**, *16*, 1951−1959.
(57) Ji, H.; Hone, D.; Pincus, P.; Rossi, G. *Macromolecules* **1990**, *23*, 698−707.
(58) Luckham, P. F.; Klein, J. *J. Chem. Soc., Faraday Trans. 1* **1984**, *80*, 865.
(59) Dahlgren, M. A. G.; Hollenberg, H. C. M.; Claesson, P. M. *Langmuir* **1995**, *11*, 4480.
(60) Dahlgren, M.; Claesson, P. M. *Prog. Colloid Polym. Sci.* **1993**, *93*, 207.
(61) Lowack, K.; Helm, C. *Macromolecules* **1998**, *31*, 823.

The division of the repulsive interaction profile between two polymer-supported bilayers into three different distance regimes is schematically shown in Figure 6:

(1) The interaction at *short distances (D < 15 nm)* is dominated by the steric repulsion of the hydrated bilayer surfaces. At higher forces, hemifusion and full fusion ($F/R \gg 80$ mN/m) can be observed.[19]

(2) In the *intermediate distance regime (D ≈ 15−40 nm)*, the polymer cushions on each surface are compressed below their equilibrium thickness. Interaction forces in this regime are therefore dominated by the elasticity of the polyelectrolyte layers.

(3) At *long distances (D > 40 nm)*, there is no direct contact between the two bilayer surfaces. The repulsive interaction in this regime most likely arises from additional (comparably weak) contributions such as entropic contributions (fluctuations, undulations) and steric effects (surface roughness), as well as from electrostatic repulsion.

The latter assumption was tested by fitting the long-range regime ($D > 40$ nm) of our force curves. Interestingly, an exponentially decaying force according to eq 3 with the parameters $A = 3.792$ mN/m and $\lambda^{-1} = 13.3$ nm fits the data recorded at low salt concentration almost exactly. While significantly different from the numbers obtained for an exponential fit in the intermediate distance regime, the latter number almost perfectly agrees with the expected Debye length of an electrostatic repulsion in 0.5 mM KNO_3 solution ($\kappa^{-1}_{(\text{theoret})} = 13.6$ nm). From the exponential prefactor, A, the magnitude of the effective surface potential, ψ_o, can be calculated,[31,62] under the assumption that the layers of effective surface charge are located at the two bilayer surfaces, which is accounted for by a Stern shift, δ, in eq 6.

$$F(D)/R = 128\pi\left[\frac{(k_B T)^3 \epsilon\epsilon_o c_s}{2e^2}\right]^{1/2} \tanh^2\left(\frac{e\psi_o}{4k_B T}\right) e^{-\kappa(D-\delta)} \quad (6)$$

in which at $T = 28$ °C, $k_B T = 4.158 \times 10^{-21}$ J, $(4k_B T/e) = 104$ mV, $(\epsilon\epsilon_o/2e^2) = 1.354 \times 10^{28}$ N^{-1} m^{-2}, and $c_s = 0.5$ mol m^{-3}. With the parameters obtained from the long-range fit, ψ_o was calculated for $\delta = D^{(o)} = 32$ nm (as given by the hydrodynamic layer thickness) as well as for $\delta = D^{(o)}_{\text{spring}} = 38.4$ nm. The resulting absolute values for the surface potential are $\psi_o = 23.5$ mV and $\psi_{o,\text{spring}} = 18.4$ mV, respectively, and we find that these absolute numbers compare well with recent ζ-potential measurements on PC liposomes in NaCl solution, in which negative values between −20 and −10 mV were determined for salt concentrations between 10^{-4} and 10^{-3} M, respectively.[63] While the presence of an electrostatic repulsion for a bilayer surface exposing the zwitterionic and thus electroneutral choline headgroups may seem somewhat counterintuitive at first sight, note that according to the Grahame equation,[31] a surface potential of 20 mV in 0.5 mM 1:1 electrolyte buffer corresponds to a surface charge of 10^{-3} C m^{-2}, that is, only one electronic charge per 160 nm^2 (or one electronic charge per approximately 250 lipid molecules). Unfortunately, the values obtained for different force curves measured under high-salt conditions have not been found as consistent as those obtained for the low-salt conditions. The determined decay lengths average $\lambda^{-1} \approx 4$ nm (instead of the expected 0.8 nm), but for a comparable surface charge density a surface potential of only $\psi_o = 1.2$ mV would be expected.[31] This would apparently result in forces too weak to be detected here. For a clear attribution of the long-range regime to the various possible contributions discussed above, a further evaluation of the long-range interaction profile at intermediate salt concentrations would therefore be needed.

As discussed earlier for the short-range interactions of polymer-supported lipid bilayers,[19] PEI-supported lipid membranes resemble freely suspended bilayers (e.g., as found in lipid vesicles) more closely than lipid membranes on solid mica supports. This feature is attributed to the swollen polyelectrolyte cushion which effectively "holds" the lipid membrane at the surface but allows it to retain its natural properties as the hydrated polymer provides an aqueous compartment between the mica substrate and the proximal lipid layer. This concept has often been compared with the cytoskeletal support in living cells.[64] Of course, the polyelectrolyte cushion of the simple model systems investigated here is by no means comparable with the complexity and functionality of the cytoskeleton. Nevertheless, the effective Young's moduli, E_{eff}, obtained from our fits are not only of the same order as the values given for thin layers of other water-swollen polymer gels such as gelatine or dextran[42,65] but are also comparable with the elastic properties of eucaryotic cells. In recent AFM measurements, their elastic moduli were found to vary between $E = 1$ and 100 kPa.[66−68]

Conclusions

In summary, the presence of an underlying water-swollen polymer cushion completely changes the interaction profile between lipid bilayer membranes. In earlier work, it had been shown already that the conserved fluidity within the lipid bilayer is most significant to their short-range interaction profile as it allows for full fusion and subsequent healing of previously fused membranes. Here, the focus has been on the long-range interaction regime; the soft support adds a strong repulsive component in the intermediate regime, in which the bilayer surfaces are in close contact. The major contribution to this repulsive component was found to be the elastic compression of the aqueous polyelectrolyte layer, which is apparently accompanied by water release from the polymeric cushion. The elastic properties and the structural parameters of the surface-bound bilayer system could be obtained from simple theoretical models. The effective Young's moduli of the polymer-supported membranes are comparable to those of living cells, and the structural data from the SFA measurements are in good agreement with independent studies by X-ray or neutron reflectometry. Additional electrostatic repulsive contributions to the interaction profile of the zwitterionic lipid membranes at large intersurface separations are expectedly weak and in agreement with findings on free vesicle systems. In summary, our experiments provide strong evidence that the aqueous polyelectrolyte cushion allows for the fixation of a lipid bilayer on a solid substrate, while retaining its natural properties as in freely suspended bilayers. This is an important requirement if surface-attached bilayers are to be used as model membranes for biophysical studies and possible biosensor applications in the future.

(62) Israelachvili, J. N.; Adams, G. E. *J. Chem. Soc., Faraday Trans. 1* **1978**, 975−1001.
(63) Egawa, H.; Furusawa, K. *Langmuir* **1999**, *15*, 1660−1666.
(64) Jacobson, K.; Sheets, E. D.; Simson, R. *Science* **1995**, *268*, 1441−1442.
(65) Domke, J.; Radmacher, M. *Langmuir* **1998**, *14*, 3320−3325.
(66) Weisenhorn, A. L.; Khorsandi, M.; Kasas, S.; Gotozos, V.; Celio, M. R.; Butt, H. J. *Nanotechnology* **1993**, *4*, 106−113.
(67) Radmacher, M.; Fritz, M.; Kacher, C. M.; Cleveland, J. P.; Hansma, P. K. *Biophys. J.* **1996**, *70*, 556−567.
(68) Radmacher, M. *IEEE Engr. Med. Biol.* **1997**, *16*, 47−57.

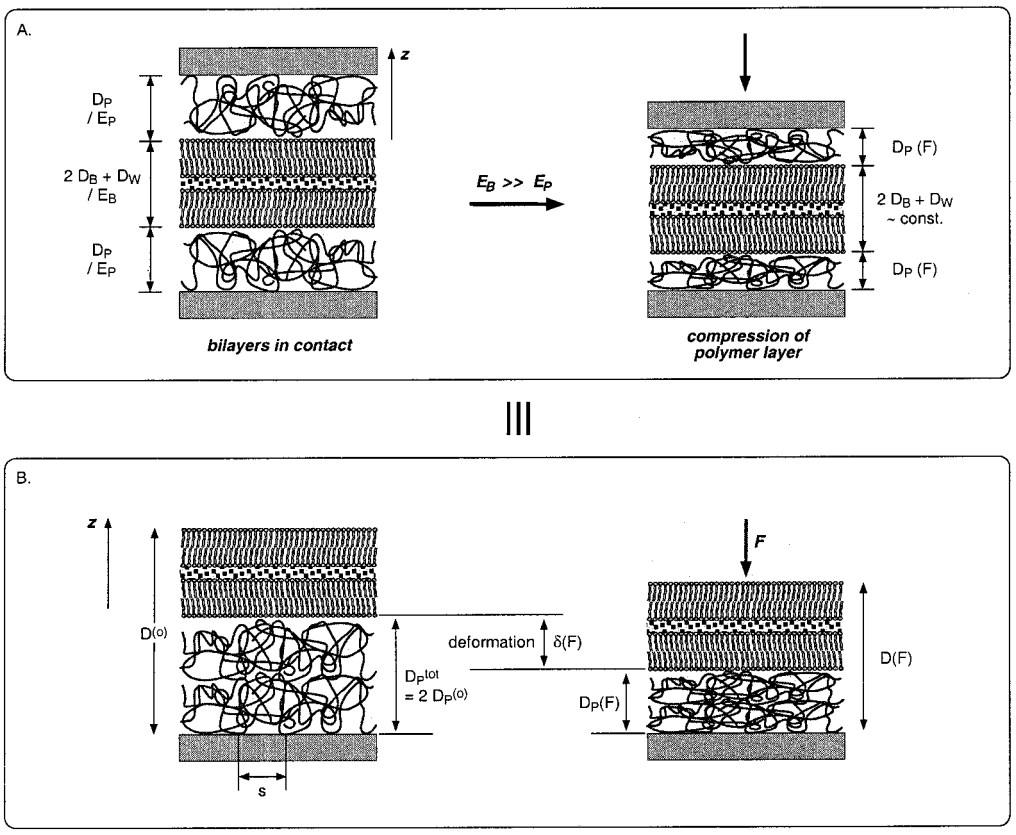

Figure 7. Analogy between a system of two interacting polymer-supported bilayer membranes investigated in static SFA experiments (case A) and a system of two contacting DMPC bilayers resting on one polymer cushion of thickness D_P^{tot} (case B) which can be described by a simple spring model (according to ref 42).

Acknowledgment. This work was supported by the National Institutes of Health (NIH) under Grant GM 47334 and by a NRSA individual postdoctoral fellowship GM17876 (J.Y.W.). M.S. was partially funded by a postdoctoral fellowship of the Deutsche Forschungsgemeinschaft (Se 855/1-1). The authors thank one of the reviewers for his critical and insightful comments, which have significantly contributed to our interpretation of the observed force hysteresis.

Appendix

Simple Spring Model. In a simple spring model, the polymer layer can be treated as a spring which is compressed in the vertical direction. This model has been introduced by Kühner and Sackmann to describe the elastic properties of dextran layers on a microscopic level.[42] Here, we briefly discuss the adaptation of this model for the description of two interacting polymer-cushioned bilayer membranes.

The symmetric case of two interacting PEI-supported DMPC bilayers is illustrated in Figure 7. For our calculation, it will be assumed that the rigidity of two DMPC bilayers in contact (separated only by one layer of hydration water) is significantly larger than that of the two polyethylenimine layers.[39] In this picture, undulations and other local fluctuations in layer thickness should be suppressed,[50] and the interface between the two can be assumed to be a "rigid" plane. No other deformation of the surfaces other than unidirectional compression in the vertical direction (*z*-axis) is assumed.[43] Furthermore, for ease of calculation, the real (symmetric) system of two polymer-supported lipid bilayer membranes (Figure 7A) is theoretically treated as the equivalent asymmetric case

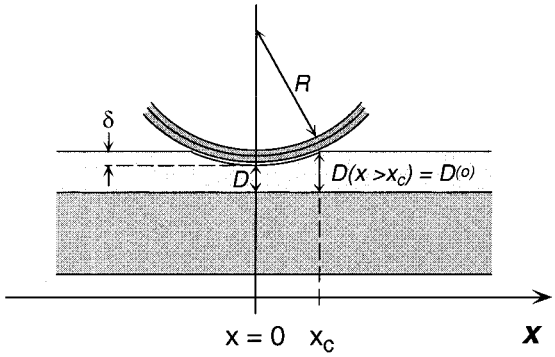

Figure 8. Simple spring model: definition of cutoff distance, x_C, and relevant parameters.

of two identical contacting bilayers compressing one PEI layer of double initial thickness $D_P^{tot} = 2D_P^{(o)}$, by means of an externally applied force, F, as shown in Figure 7B. On this basis, our approach is then practically identical to the simple spring model introduced by Kühner and Sackmann for the description of a latex bead hovering over a thin dextran film.[42]

Briefly, for a homogeneous compression in the normal direction (*z*-axis), the total deformation, $\delta(F)$, is given by $\delta = pD_P^{tot}/E_P$ where p is the disjoining pressure and E_P is the elastic modulus of the polymeric film. Because in the described SFA measurements the two surfaces interact in a crossed cylinder geometry, the expression above is converted from planar to curved geometry by the Derjaguin approximation,[31] which gives the force between a spherical bilayer surface interacting with a flat polymer surface (Figure 8) as a function of the polymer deformation, δ,

which in turn depends on the lateral position, x.

$$F(\delta) = \int_{x=0}^{x_c} 2\pi x p(\delta(x))\, dx$$

x_C is the lateral cutoff distance above which the elastic forces no longer contribute to the interaction between the two surfaces.[42] In our case, x_C is simply given by the radius of the contact spot, which is assumed to be constant in the intermediate distance regime (this assumption was found to be valid in the experiments). For $\delta \ll R$ and therefore $x_C^2 \approx 2Rd$, the deformation of the compressed polymer region is given as $\delta(x) \approx x^2/2R$, and $F(\delta) = \pi E_P R\delta^2/D_P^{tot}$. The elastic contribution to the measured interaction profile is therefore given by

$$F(D)/R = \frac{\pi E_P}{D_P^{tot}}(D^{(o)} - D)^2$$

where $D = D^{(o)} - \delta$ is the total thickness of the system (i.e., the mica−mica separation in SFA experiments), $D^{(o)}$ is the equilibrium thickness of the total layer system (in the absence of external load), and D_p^{tot} is the combined thickness of the two polyethylenimine layers (e.g., in a symmetric SFA experiment, $D_P^{tot} = D^{(o)} - 2D_B - D_W$).

LA0103012